Published in final edited form as:
J Neuropathol Exp Neurol. 2008 September ; 67(9): 900–910. doi:10.1097/NEN.0b013e31818521cd.

Patterns of Brain Infiltration And Secondary Structure Formation in Supratentorial Ependymal Tumors

Norman L. Lehman, MD, PhD
Department of Pathology, Stanford University School of Medicine, 300 Pasteur Drive, Stanford, California

Abstract

Ependymomas are generally considered to be non-infiltrative tumors that have discrete borders with adjacent brain tissue. Most occur in the posterior fossa or spinal cord. Supratentorial ependymal tumors arise near the ventricular system, or more rarely, within the cerebral white matter or cortex. Presented here are six supratentorial ependymal tumors, three that primarily involve the cerebral cortex and three that extend into the cortex from the underlying white matter. By microscopy, all of these tumors locally infiltrate the cortex and/or white matter along small blood vessels and axonal fiber tracts. They also form other glioma secondary structures including perineuronal tumor cell satellitosis and subpial tumor cell mounds. The three cortical ependymal tumors show a spectrum of features ranging from conventional and clear cell ependymoma-like patterns to more angiocentric glioma-like histology. Since ependymal tumors generally have a significantly better prognosis than other infiltrating gliomas, recognition of their capacity to infiltrate adjacent cortex and white matter is important to prevent the misdiagnosis of oligodendroglioma, astrocytoma, or infiltrating glioma, not otherwise specified. Cortical ependymomas and angiocentric gliomas may comprise a group of locally infiltrative ependymal tumors that are associated with an excellent prognosis following gross total surgical resection.

Keywords

Angiocentric cortical ependymal tumor; Angiocentric glioma; Infiltrative; Cortical ependymoma; Secondary structures; Supratentorial ependymoma

INTRODUCTION

Classical WHO grade II ependymomas and grade III anaplastic ependymomas occur most commonly in the fourth ventricle of children and in the fourth ventricle and spinal cord of adults (1,2). Ependymomas can also be supratentorial in location and associated with the third or lateral ventricles; or they may be centered within the subcortical white matter without a direct connection to the ventricular system (3–6). Occasionally, these tumors extend into the cerebral cortex; rarely ependymomas appear to arise within the cerebral cortex and are referred to as “cortical ependymomas” (7–9).

Ependymomas are generally considered non-infiltrative tumors and are thought to exert their biological effects largely by mass effect, usually demonstrating discrete borders with neighboring brain or spinal cord (1,3). Locally infiltrative behavior, however, has been

Current address for correspondence and reprint requests: Norman L. Lehman, MD, PhD, Department of Pathology and Laboratory Medicine, Henry Ford Hospital, 2799 West Grand Boulevard, Detroit MI 48202. Telephone: (313) 916-3653; Fax: (313) 916-7120; E-mail: nllehman@yahoo.com.

occasionally recognized in posterior fossa ependymomas (2), but has not been well documented in supratentorial ependymomas.

This report concerns six supratentorial ependymal tumors. Three appeared to have extended into the cortical gray matter from the underlying white matter and three were centered within the cortical gray matter. In contrast to classical descriptions of ependymomas as non-infiltrative lesions, these tumors all demonstrated invasion within the cortical gray matter and/or subcortical white matter along axonal tracts and surrounding small blood vessels. Furthermore, like infiltrating astrocytomas and oligodendrogliomas, the infiltrating ependymoma cells formed other glial tumor secondary structures, including perineuronal satellitosis and subpial tumor cell mounds (10). The diagnostic, surgical and ontologic implications of these previously under-appreciated, potentially infiltrative characteristics of supratentorial ependymal tumors are discussed.

MATERIALS AND METHODS

Six cases of surgically resected supratentorial ependymal tumors in which recognizable portions of cortical gray matter were present within the specimen were reviewed. Specimens were fixed in 10% buffered formalin and submitted for routine processing and paraffin embedding. Hematoxylin and eosin (H&E)-stained slides were examined, and immunohistochemical stains for glial fibrillary acidic protein (GFAP), epithelial membrane antigen (EMA), Ki-67 (MIB-1 antibody), CD99, and in some cases S100 or neurofilament protein (NFP) (all antibodies from Dako, Carpinteria CA), were performed using standard immunohistochemical procedures after microwave pretreatment. Standard 3′3′-diaminobenzidine (DAB) or aminoethylcarbazole (AEC) was used as the chromogen. Ki-67 labeling indices were estimated by counting the number of MIB-1 antibody positive cells from a total of approximately 400 cells in the most proliferative areas of the tumors.

Case Histories

Case 1—Right frontal cortical ependymoma in an 11-year-old boy presenting with refractory seizures. This previously reported lesion was well circumscribed, partially cystic and minimally enhancing radiographically (Fig. 1A) (8); at surgery, it also appeared to be well circumscribed. Histologically, the noncystic portion of the tumor and the cyst walls were composed of continuous sheets and cords of tumor cells without intervening brain tissue (Fig. 1B). Tumor cells were mostly unipolar to bipolar columnar- to spindle-shaped cells and were occasionally arranged in perivascular pseudorosettes (Fig. 1C) and true ependymal rosettes (Fig. 1C inset). The tumor also exhibited clear epithelioid-like cells that were most often grouped into subpial mounds (Fig. 1B); it showed perinuclear dot and ring EMA-immunopositivity (8) and was strongly CD99- and GFAP-immunopositive (Fig. 1E, F). The Ki-67 labeling index was less than 1%. The tumor also demonstrated non-rosetting, circumferential angiocentric growth among entrapped neurons at the periphery of its major solid, sheet-like component (Fig. 1C, D). The patient was treated with gross total resection and has been recurrence- and seizure-free for 7 years. The clinical features of this and the other five cases are summarized in the Table.

Case 2—Right frontal cortical ependymoma in a 1-year-old girl who presented with refractory seizures. On imaging, the tumor appeared to be a well-circumscribed 6.0 × 6.0 mm, T1 isointense, slightly T2 hyperintense, nonenhancing solid mass. Follow-up neuroimaging 6 months later revealed enlargement of the lesion (Fig. 2A) and surgery was performed. Histologically, the tumor demonstrated GFAP-immunopositive clear cells aggregated in dense nodules and subpial mounds, occasional perivascular pseudorosettes and rare ependymal rosettes (Fig. 2B–E). Rare focal perinuclear dot-pattern EMA immunopositivity was observed.

Although the lesion was grossly well circumscribed, microscopically it was locally infiltrative. It showed GFAP-immunopositive non-rosetting angiocentric growth, tumor cell perineuronal satellitosis and free neoplastic cells infiltrating the neuropil at the tumor periphery (Fig. 2F, G). The dense tumor nodules showed conspicuous mitotic activity and a very high Ki-67 labeling index of 50% to 80%. The Ki-67 labeling index was also relatively high in other areas of the lesion at 8% to 15% (Fig. 2H). No vascular proliferation or necrosis was present. The tumor was excised and despite the high proliferation index, the patient has remained free of seizure and recurrence for four years.

Case 3—Right temporal tumor in a 47-year-old man with a 23-year history of poorly controlled complex partial seizures. MRI revealed a T1 isointense, T2 hyperintense, nonenhancing lesion involving the right medial temporal lobe in the region of the amygdala (Fig. 3A). Surgical resection eliminated the patient's seizures, but they returned approximately one year later. He refused a second surgery and was lost to follow-up.

Histologically, the tumor was composed of unipolar and bipolar spindle-shaped and occasionally clear epithelioid-shaped cells with round to oval nuclei containing stippled chromatin. Tumor cells were present in both solid and locally infiltrative components (Fig. 3B–E). The lesion demonstrated perivascular pseudorosettes, circumferential angiocentric spread along small blood vessels, subpial clear cell mounds, and rare ependymal rosettes (Fig. 3C–E). Tumor cells were GFAP- and CD99-immunopositive (Fig. 3F, G). Many contained EMA-immunopositive intracellular microlumina and perinuclear dot EMA immunopositivity (Fig. 3E). The Ki-67 labeling index was less than 1%. As in the two cases described above, cortical neurons appeared entrapped in less dense areas (Fig. 3C–E, H). In infiltrative zones of the tumor, neoplastic cells associated with distinct perivascular pseudorosettes were occasionally observed, apparently in transition to a non-rosetting angiocentric spread (Fig. 3D, H).

Case 4—Right temporal lobe tumor in a 2-year-old male with an approximately 10-month history of progressive left arm and leg paraplegia. Imaging showed an enhancing 6.5-cm partially cystic tumor involving the right temporal lobe and lateral ventricle extending into the basal ganglia, thalamus, midbrain and inferior medial temporal cortex. The center of the tumor was hyperintense in T2 images (Fig. 4A). Microscopically, the tumor had a mixed classic ependymoma and clear cell ependymoma histology with a solid, sheet-like growth pattern, occasional calcifications and numerous perivascular pseudorosettes (Fig. 4B, C). The neoplasm invaded adjacent white matter and the overlying cortex along axonal tracts and to a lesser extent in an angiocentric pattern (Fig. 4D–F). It also exhibited perineuronal satellitosis and individual infiltrating tumor cells (Fig. 4D–E). The tumor was intensely GFAP-immunopositive, displayed perinuclear dot-like EMA immunoreactivity and was also strongly CD99-immunopositive (Fig. 4G–I). The Ki-67 labeling index was approximately 3%. No mitotic activity, endothelial cell proliferation or necrosis was appreciated. The patient was treated with local field radiation therapy. Two years after surgery he showed no evidence of recurrence.

Case 5—Left frontal lobe tumor in an 8-year-old boy presenting with a generalized tonic-clonic seizure preceded by a 3-day history of headache, nausea and vomiting. MRI showed an approximately 8.4 × 8.0 cm heterogeneously enhancing transmantle mass with focal mineralization and cavitary changes (Fig. 5A). H&E-stained sections revealed a dense glioma centered deep in the cerebral white matter (Fig. 5B). It contained occasional true ependymal rosettes and perivascular pseudorosettes (Fig. 5C, D). The tumor cells had mostly round nuclei with evenly distributed chromatin. The cytoplasmic borders often were halo-like (i.e. clear cell histology), but sometimes contained faint granular cytoplasm (Fig. 5E). Dense cellular nodules with increased mitotic figures and small areas of necrosis were noted, as were scattered calcospherites (Fig. 5B).

Overall, the tumor showed patchy moderate GFAP immunoreactivity but occasional tumor cells exhibited strong GFAP immunopositivity (Fig. 5F). A CD99 immunostain showed an intracytoplasmic dot pattern. An EMA immunostain showed equivocal perinuclear dot immunopositivity. The Ki-67 labeling index was 20%. Neoplastic cells appeared to infiltrate the cortex individually, sometimes as perineuronal satellites or in linear groups, and occasionally along blood vessels in a distinct but non-rosetting manner (Fig. 5E, G, I). Neurofilament protein (NFP) immunostaining revealed that tumor cells infiltrated into the cerebral cortex between neuron fibers (Fig. 5J–K). In some areas, the tumor extended to the pial surface in a continuous sheet-like manner and in others the tumor cells formed subpial mounds (Fig. 5L). A gross total resection was performed and the patient was subsequently treated with local field radiation therapy. He has since done well one year after surgery.

Case 6—Left frontoparietal tumor in a 12-year-old girl. This large solid, T2-hyperintense tumor is a recurrence of an ependymoma resected two years and 4 months earlier when the patient was 8 years old (Fig. 6A). No other therapy was performed at that time. The surgical specimen of the recurrent tumor consisted of multiple CUSA fragments of a highly cellular neoplasm that involved brain tissue (Fig. 6B–G). Clear cell histology was present in some areas, as were occasional indistinct perivascular pseudorosettes; true ependymal rosettes were absent (Fig. 6B–D). Mineralization was present in the form of occasional calcospherites and mineralized small blood vessels (Fig. 6D–G). The lesion cells were immunoreactive for S100, but negative for GFAP and EMA. They did, however, show strong membrane staining for CD99 (Fig. 6H). Only rare mitotic figures were found and the Ki67 labeling index was 10%. Vascular proliferation and necrosis were not seen. The tumor was present in the subarachnoid space and appeared to extend into Virchow-Robin spaces (Fig. 6F). Cortical tissue showed single infiltrating tumor cells in the parenchyma, occasional tumor cells infiltrating along small capillaries and perineuronal satellitosis (Fig. 6E–G). Due to the highly fragmented nature of the specimen it was not possible to determine if the cortex was infiltrated from below by deep tumor or from above by tumor within the subarachnoid space. The patient was treated with local field radiation therapy and the tumor has not since recurred. She is doing well now six years after her original diagnosis.

DISCUSSION

Classic cellular features of ependymomas include round to oval nuclei with evenly dispersed stippled chromatin, perivascular pseudorosettes, true ependymal rosettes, and frequent immunoreactivity for GFAP, S100, CD99 (MIC-2) and EMA, the latter often in a perinuclear dot and/or ring pattern (1,11,12). With the exception of the cellular ependymoma (case 6), the cases described here demonstrated most of these features and all expressed CD99 in a strong membranous, diffuse cytoplasmic or cytoplasmic dot pattern; this reactivity is highly specific for differentiating ependymomas from other CNS tumors (13). Additionally, all of the cases showed infiltrating individual tumor cells in the parenchyma and non-rosetting angiocentric spread along small cerebral blood vessels. In addition to angiocentric growth, these lesions also exhibited infiltration along axonal tracts, perineuronal satellitosis, and subpial mounding, i.e. the classic secondary structures also found in high-grade astrocytomas and oligodendrogliomas (10). These findings are in contrast to the general dogma that ependymal tumors are non-infiltrative lesions. Unlike in “diffusely infiltrative” gliomas, however, the infiltration demonstrated by these six supratentorial ependymal tumors appeared to be mostly locally infiltrative, i.e. confined to areas at the periphery of the main tumor masses.

Non-rosetting angiocentric growth in ependymal tumors may reflect the ontologic affinity of neoplastic ependymal cells to make contact with blood vessels similar to ependymal tanycytes (14,15). This pattern is, therefore, likely biologically related to perivascular pseudorosetting, perhaps depending on the state of differentiation of the ependymal cell, i.e. tanycyte-like versus

polygonal (12). Although the tumors in this series demonstrated numerous ependymal features, it is important to note that neoplastic astrocytes may also form perivascular rosette-like structures (gliovascular structures) and form tumor secondary structures.

An apparent direct transition from perivascular pseudorosette formation to nonrosetting angiocentric growth could be observed in these supratentorial ependymal tumors (Fig. 3D, H). In some instances, tumor cell angiocentricity may simply reflect a path of least resistance for infiltrating tumor cells (tumor secondary structure). The latter may be observed as spread within the Virchow-Robin space after subarachnoid extension (Fig. 6F).

The relative rarity of ependymomas that secondarily involve the cerebral cortex, and pure cortical ependymal tumors, may in part account for the under-recognition of the non-rosetting angiocentric growth pattern in ependymomas. Other possible factors include the fragmented nature, or poor histological preservation of the small cortical fragments in CUSA specimens. The paucity of cortical tissue surrounding the tumor in typical ependymoma surgical specimens may be another cause. Indeed, the standard neurosurgical approach to the resection of ependymomas is to “shell them out” without routinely obtaining a significant margin of uninvolved tissue. Indeed, in a retrospective examination of three previously reported cases of cortical ependymoma (9), cortical tissue was present in only one specimen and that small fragment showed free tumor cell infiltration. Furthermore, there might be an observational bias towards the non-infiltrative behavior of ependymomas resulting in an under recognition of tumor cell spread or invasion in cortical fragments.

Remarkably, although the tumor in case 2 showed a very high Ki-67 labeling index, it has not recurred (Table). Proliferative index and extent of tumor resection have been statistically shown to be important independent prognostic indicators in intracranial ependymomas (1,3–5,16,17). In supratentorial ependymal tumors, however, proliferative index may not be as important as an independent prognostic factor (4,6), particularly in tumors limited to the cortex and immediately underlying white matter.

It is also noteworthy that, although locally infiltrative, at least two of the cortical ependymal tumors with long-term follow-up in this series (cases 1, 2) appear to have been surgically cured; in both cases a margin of relatively normal cortex was obtained. In contrast, one cortical tumor (case 3) and one transmantle tumor (case 6) recurred following resection, although the latter may have been cured by repeat resection and radiation therapy (Table). Hence, a surgical margin of several millimeters or more, when possible, in the surrounding uninvolved cerebral tissue to include any tissue of abnormal color or texture may encompass most of the tissue involved by local infiltration. This might better prevent recurrence in select cases of supratentorial ependymal tumors compared to a gross total resection involving a less aggressive effort to achieve a clear surgical margin.

Angiocentic gliomas, previously known as angiocentric neuroepithelial tumors (ANETs) and monomorphous angiocentric gliomas, are recently described cortical tumors of ependymal differentiation characterized by perivascular cuffing of tumor cells in a circumferential or non-rosetting angiocentric infiltrative growth pattern similar to as observed in the ependymal tumors described herein. Angiocentric gliomas are composed of GFAP-immunopositive cells, sometimes arranged in perivascular pseudorosettes. In many cases they demonstrate perinuclear dot EMA immunoreactivity and ependymal ultrastructural features. Like cortical ependymomas, angiocentric gliomas occasionally show spindle cells arranged in schwannoma-like fascicles (Fig. 3B), small polyhedral cells, and larger epithelioid cells often in subpial mounds (8,9,18–20).

Preusser et al found 6q24 to q25 loss as the only chromosomal abnormality in one of eight cases of angiocentric glioma by comparative chromosomal genomic hybridization (21). This

is further suggestive evidence that angiocentric gliomas are closely related to classic ependymomas since 6q loss is common in ependymomas. Indeed, Huang et al found 6q24 to q25.3 loss to be the most frequent chromosomal aberration in their series of 30 ependymomas (22).

Like angiocentric gliomas, all three cases of cortical ependymal tumors described above had various amounts of non-rosetting angiocentric spread along small blood vessels and variable amounts of compact or solid tumor growth. As described for those tumors originally termed ANETs (18), two of the cortical ependymal tumors (cases 1 and 2) showed very small amounts of white matter involvement. Although entrapped or displaced cortical neurons were found outside of the solid components of the three cortical tumors presented above, no definite neuronal component was observed in any of the solid areas of these tumors. This suggests that the involved neurons are not part of the neoplasms; this was offered as an alternative hypothesis for neurons found associated with ANETs by Lellouch-Tubiana et al (18). Furthermore, in a recent study of neuronal differentiation in ependymomas, neuronal differentiation was expressed as either neurocytic cells within neuropil islands or desmoplastic medulloblastoma-like pale islands, or as cells scattered throughout the tumors with only immunohistochemical or limited ultrastructural neurocytic features (23). No mature neuronal or ganglionic appearing cells were reported. Nevertheless, since most cortical ependymomas and angiocentric gliomas initially present as seizures in children, they are likely congenital in nature and some degree of cortical dysplasia might be linked to their histogenesis.

Case 3 can be categorized as an angiocentric glioma. The cortical ependymal tumors represented by cases 1 and 2 show some similarities to angiocentric gliomas as they demonstrate angiocentric parenchymal infiltration, but differ from angiocentric gliomas by their more extensive solid tumor components and other variable morphological features. Both cortical ependymomas and angiocentric gliomas are associated with a very good surgical prognosis (8,9,18–20). Angiocentric gliomas are described as being “of uncertain relationship to other neoplasms exhibiting ependymal differentiation” in the current WHO classification (20). The overlapping histocytologic features and biological behavior of angiocentric gliomas and cortical ependymomas suggests, however, that they could both be considered as entities within a spectrum of clinically low-grade, cortical ependymal tumors. These tumors may also show overlapping histologic and clinical features with low-grade cortical astroblastomas in children (12).

It is not clear when a tumor should be subclassified as a cortical ependymoma or an angiocentric cortical ependymal tumor (ACET) (angiocentric glioma) (12,24). The classification should, perhaps, be based on the percentage of solid versus infiltrating angiocentric components. Nevertheless, satisfactory histological criteria for distinguishing between these two entities will likely require clinical, morphological and perhaps molecular studies of a larger series of cortical ependymal tumors. Both lesions show a very low proliferative index and this is likely an important criterion, if not for distinguishing between the two, but perhaps for making the general diagnosis of cortical ependymal tumor (8,9,18–20).

Although most ependymal tumors exhibit limited infiltrative behavior, pathologists should be aware of their potential infiltrative nature to avoid the misdiagnosis of other types infiltrating gliomas. This is particularly pertinent in differentiating supratentorial infiltrating clear cell ependymomas from oligodendrogliomas, since they may closely resemble each other both cytologically (perinuclear halos or clear cells) and architecturally (secondary structures).

Infiltrating supratentorial ependymal tumors have likely sometimes previously been generically labeled “infiltrating gliomas.” Because the most important prognostic factor for ependymal tumors is extent of resection, it is essential to alert clinicians to the ependymal

nature of these neoplasms so that attempts at gross total resection can be made whenever possible. Lastly, recognition of the potential infiltrative nature of supratentorial ependymal tumors may have important implications for future tumor classification and prediction of their biological behavior and response to adjunctive treatment.

Acknowledgments

Supported by Grant No. K08 NS45077 from the National Institute of Neurological Disorders and Stroke.

The author thanks Dr. Michael Edwards, Dr. Stephen Huhn and Dr. Steven Fulop for clinical follow-up information; Dr. Mark Cohen of Case Western Reserve University (Cleveland, OH) for slides of case 3; Dr. Hernan Molina-Kirsch of the Laboratorio de Patologia (Guatemala City, Guatemala) for slides of case 6 and Dr. Federico Roncaroli of the Imperial College of London, Charing Cross Hospital (London, UK) for providing slides of his 3 previously published cases of cortical ependymoma for review (9); and Dr. Bernd Scheithauer for reviewing case 6. I also thank Dr. Terri Haddix and Dr. Patrick Barnes for radiology images; Dr. Federico Roncaroli, Dr. Mohanpal Dulai and Dr. Jorge Gutierrez for invaluable comments; and Martin Estrada, Kathy Roszka, Monica Grenke and Nancy Lemke for expert histology technical services.

References

1. McLendon, RE.; Wiestler, OD.; Kros, JM., et al. Ependymoma. World Health Organization Classification of Tumours. In: Louis, DN.; Ohgaki, H.; Wiestler, OD.; Cavenee, WK., editors. WHO Classification of Tumors of the Central Tumors of the Nervous System. Vol. 4. Lyon, France: IARC Press; 2007. p. 74-78.
2. Ferrante L, Mastronardi L, Schettini G, et al. Fourth ventricle ependymomas. A study of 20 cases with survival analysis. Acta Neurochir (Wien) 1994;131:67–74. [PubMed: 7709787]
3. Palma L, Celli P, Mariottini A, et al. The importance of surgery in supratentorial ependymomas. Long-term survival in a series of 23 cases. Childs Nerv Syst 2000;16:170–55. [PubMed: 10804053]
4. Schwartz TH, Kim S, Glick RS, et al. Supratentorial ependymomas in adult patients. Neurosurgery 1999;44:721–31. [PubMed: 10201296]
5. Vinchon M, Soto-Ares G, Riffaud L, et al. Supratentorial ependymoma in children. Pediatr Neurosurg 2001;34:77–87. [PubMed: 11287807]
6. Shuangshoti S, Rushing EJ, Mena H, et al. Supratentorial extraventricular ependymal neoplasms: a clinicopathologic study of 32 patients. Cancer 2005;103:2598–2605. [PubMed: 15861411]
7. Fujimoto K, Ohnishi H, Koshimae N, et al. Brain surface clear cell ependymoma: Case report. No Shinkei Geka 1999;27:843–46. [PubMed: 10478346]
8. Lehman NL, Jorden MA, Huhn SL, et al. Cortical ependymoma. A case report and review. Pediatr Neurosurg 2003;39:50–54. [PubMed: 12784079]
9. Roncaroli F, Consales A, Fioravanti A, et al. Supratentorial cortical ependymoma: Report of three cases. Neurosurgery 2005;57:E192. [PubMed: 15987557]
10. Reifenberger, G.; Kros, JM.; Louis, DN., et al. Oligodendroglioma. World Health Organization Classification of Tumours. In: Louis, DN.; Ohgaki, H.; Wiestler, OD.; Cavenee, WK., editors. WHO Classification of Tumors of the Central Tumors of the Nervous System. Vol. 4. Lyon, France: IARC Press; 2007. p. 54-59.
11. Kawano N, Yasui Y, Utsuki S, et al. Light microscopic demonstration of the microlumen of ependymoma: A study of the usefulness of antigen retrieval for epithelial membrane antigen (EMA) immunostaining. Brain Tumor Pathol 2004;21:17–21. [PubMed: 15696964]
12. Lehman NL. CNS tumors with ependymal features: A broadened spectrum of primarily ependymal differentiation? J Neuropathol Exp Neurol 2008;67:177–88. [PubMed: 18344909]
13. Choi YL, Chi JG, Suh YL. CD99 immunoreactivity in ependymoma. Appl Immunohistochem Mol Morphol 2001;9:125–29. [PubMed: 11396629]
14. Friede RL, Pollack A. The cytogenetic basis for classifying ependymonas. J Neuropathol Exp Neurol 1978;137:103–18. [PubMed: 632843]
15. Flament-Durand J, Brion JP. Tanycytes: Morphology and functions: A review. Int Rev Cytol 1985;96:121–55. [PubMed: 2416706]

16. Wolfsberger S, Fischer I, Hoftberger R, et al. Ki-67 immunolabeling index is an accurate predictor of outcome in patients with intracranial ependymoma. Am J Surg Pathol 2004;28:914–20. [PubMed: 15223962]

17. Kurt E, Zheng PP, Hop WC, et al. Identification of relevant prognostic histopathologic features in 69 intracranial ependymomas, excluding myxopapillary ependymomas and subependymomas. Cancer 2006;106:388–95. [PubMed: 16342252]

18. Lellouch-Tubiana A, Boddaert N, Bourgeois M, et al. Angiocentric neuroepithelial tumor (ANET): A new epilepsy-related clinicopathological entity with distinctive MRI. Brain Pathol 2005;15:281–86. [PubMed: 16389940]

19. Wang M, Tihan T, Rojiani AM, et al. Monomorphous angiocentric glioma: A distinctive epileptogenic neoplasm with features of infiltrating astrocytoma and ependymoma. J Neuropathol Exp Neurol 2005;64:875–81. [PubMed: 16215459]

20. Burger, PC.; Jouvet, A.; Preusser, M., et al. Angiocentric glioma. World Health Organization Classification of Tumours. In: Louis, DN.; Ohgaki, H.; Wiestler, OD.; Cavenee, WK., editors. WHO Classification of Tumors of the Central Tumors of the Nervous System. Vol. 4. Lyon, France: IARC Press; 2007. p. 92-93.

21. Preusser M, Hoischen A, Novak K, et al. Angiocentric glioma: report of clinico-pathologic and genetic findings in 8 cases. Am J Surg Pathol 2007;31:1709–18. [PubMed: 18059228]

22. Huang B, Starostik P, Schraut H, et al. Human ependymomas reveal frequent deletions on chromosome 6 and 9. Acta Neuropathol 2003;106:357–62. [PubMed: 12898154]

23. Rodriguez FJ, Scheithauer BW, Robbins PD, et al. Ependymomas with neuronal differentiation: A morphologic and immunohistochemical spectrum. Acta Neuropathol (Berl) 2007;113:313–24. [PubMed: 17061076]

24. Lum DJ, Halliday W, Watson M, et al. Cortical ependymoma or monomorphous angiocentric glioma? Neuropathology 2008;28:81–86. [PubMed: 18021197]

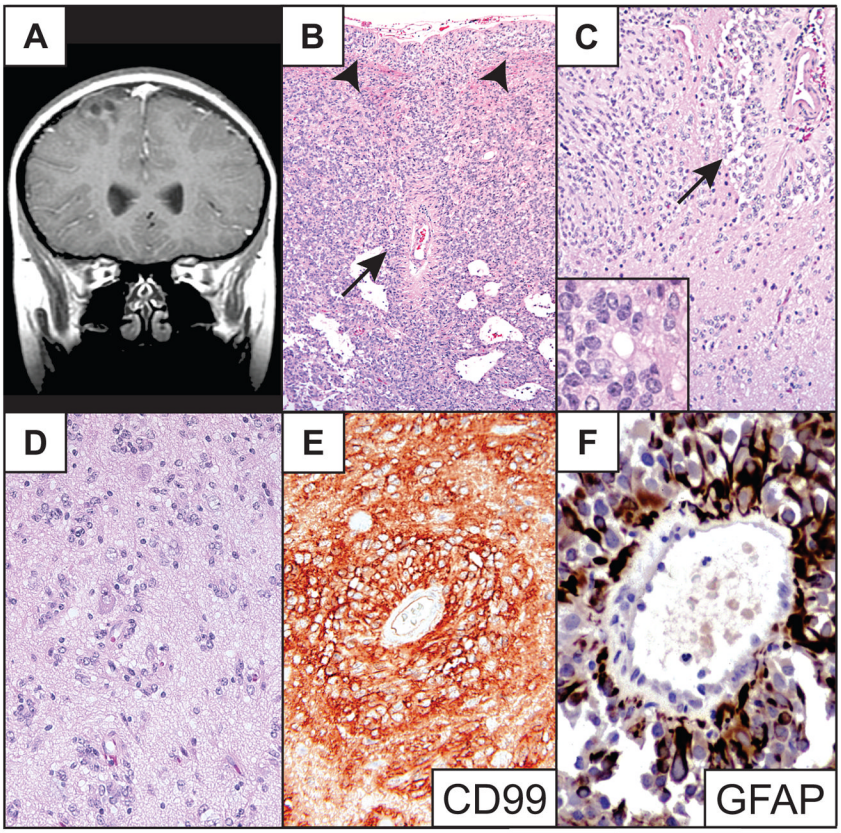

Fig 1.

Patient 1. **(A)** Coronal T1-weighted MR image of the partially cystic cortical tumor. **(B)** Low-power photomicrograph of a representative portion of tumor. Note subpial mounding of tumor cells (arrowheads) and a perivascular pseudorosette (arrow). **(C)** The periphery of the tumor demonstrates a locally infiltrative border. A large perivascular pseudorosette (arrow), numerous nonrosetting angiocentric structures and a true ependymal rosette (inset) are shown. **(D)** High-power photomicrograph of nonrosetting angiocentric infiltration among cortical neurons. **(E)** Immunostain shows strong tumor cell membrane CD99 immunoreactivity. **(F)** Glial fibrillary acidic protein (GFAP) immunostain highlights a perivascular pseudorosette demonstrating strong GFAP immunoreactivity. Routine stains are hematoxylin and eosin. Original magnifications: **(B)** 100×; **(C, E)** 200×; **(C inset, F)** 600×; **(D)** 400×.

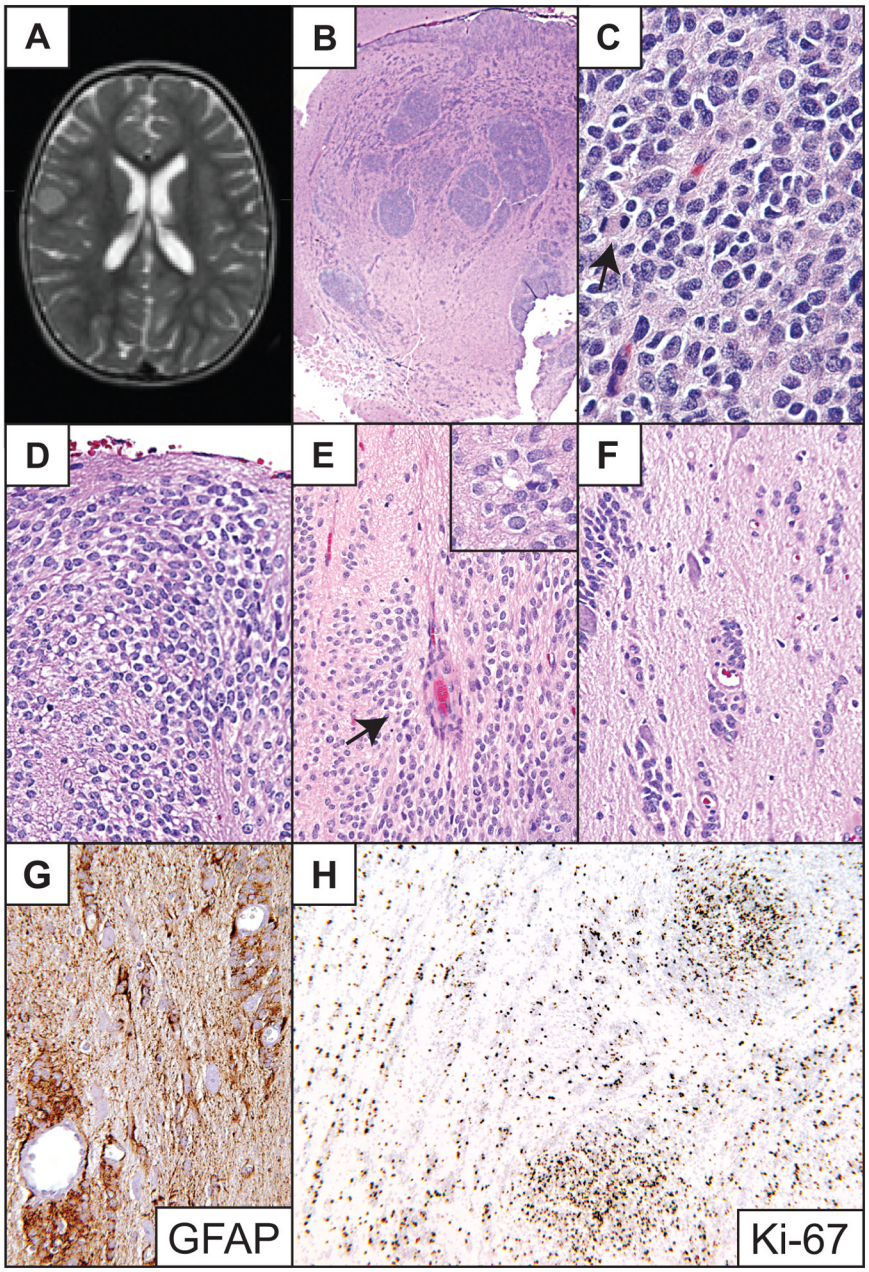

Fig 2.

Patient 2. **(A)** T2-weighted MR image illustrates slightly hyperintense lesion centered in the cerebral cortex. **(B)** Low-power image of the tumor demonstrates numerous densely cellular nodules and focal disruption of underlying white matter. **(C)** High-power photomicrograph of the dense tumor cell nodules. A mitotic figure (anaphase) is visible on the left (arrow). **(D)** The tumor formed subpial mounds of clear epithelioid cells. **(E)** Both pseudorosettes (arrow) and true rosettes (inset) were present. **(F, G)** Tumor cells infiltrated freely and along small blood vessels in a non-rosetting pattern, and also along neurons, most strikingly at the periphery of the lesion. **(H)** The dense tumor cell nodules showed a Ki-67 labeling index of 50 to 80%. Hematoxylin and eosin stains, except **(G)** and **(H)**, which are GFAP and Ki-67 immunoperoxidase stains, respectively. Original magnifications: **(B)** 20×; (**C)** 600×; **(D, E** inset**)**; 400×; **(E–G)**; 200×; **(H)** 100×.

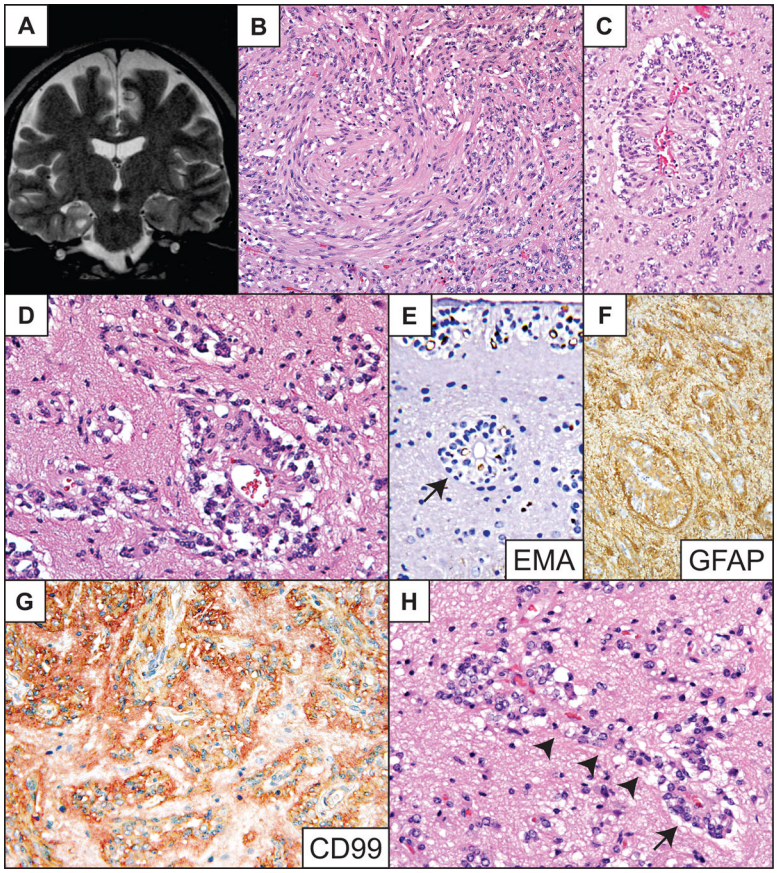

Fig 3.

Patient 3. **(A)** T2-weighted coronal MR image showing T2 hyperintense tumor in the right amygdala region. **(B)** Medium-power photomicrograph showing the solid component of the tumor and a spindle cell pattern. **(C, D)** Higher-power images demonstrating perivascular pseudorosettes, nonrosetting angiocentric growth centered on numerous capillaries, and freely infiltrating tumor cells in the parenchyma. **(E)** Epithelial membrane antigen (EMA) immunostain highlights tumor cells in a dot and ring pattern among single parenchymal tumor cells, nonrosetting angiocentric structures, true ependymal rosettes (arrow) and subpial mounds (upper portion of field). **(F, G)** The tumor is intensely glial fibrillary acidic protein (GFAP) (**F**) and CD99 (**G**) immunopositive. **(H)** High-power shows tumor cells in apparent transition from a radial perivascular pseudorosette arrangement (arrow) to circumferential nonrosetting angiocentric growth (arrowheads). Routine stains are hematoxylin and eosin. Original magnifications: **(B, C, F)** 200×; **(E, G)** 400×; **(D, H)** 600×.

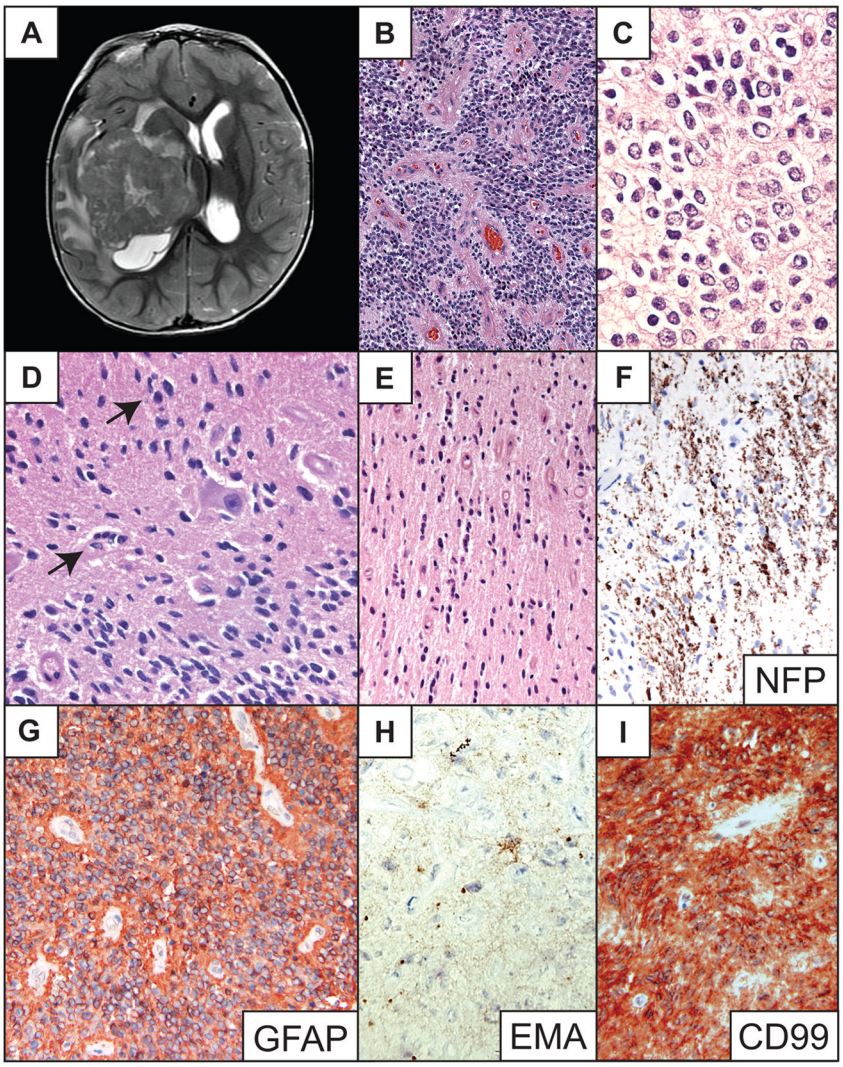

Fig 4.

Patient 4. **(A)** T2-weighted, post-gadolinium axial MR image of right hemispheric tumor. **(B)** Low-power photomicrograph of representative area of main tumor mass shows a densely cellular ependymoma with numerous perivascular pseudorosettes around slightly hyalinized vessels. **(C)** Magnified view of clear cell cytology. **(D)** High-power photomicrograph showing focal nonrosetting angiocentric spread (arrows) and perineuronal satellitosis by tumor cells. **(E)** Individual tumor cells infiltrate along white matter tracts, and to a lesser extent around small blood vessels. **(F)** Neurofilament protein (NFP) immunostain demonstrates axons surrounded by infiltrating tumor cells. **(G)** Immunostain depicts strong tumor glial fibrillary acidic protein (GFAP) immunopositivity. (**H)** Tumor cells show dot-like epithelial membrane antigen (EMA) immunoreactivity. (**I)** The tumor also demonstrates diffuse strong membranous CD99 immunopositivity. Hematoxylin and eosin stains, except where otherwise indicated. Original magnifications: **(B)** 100×; **(C, H)** 600×; **(E, F, G, I)** 200×; **(D)** 400×.

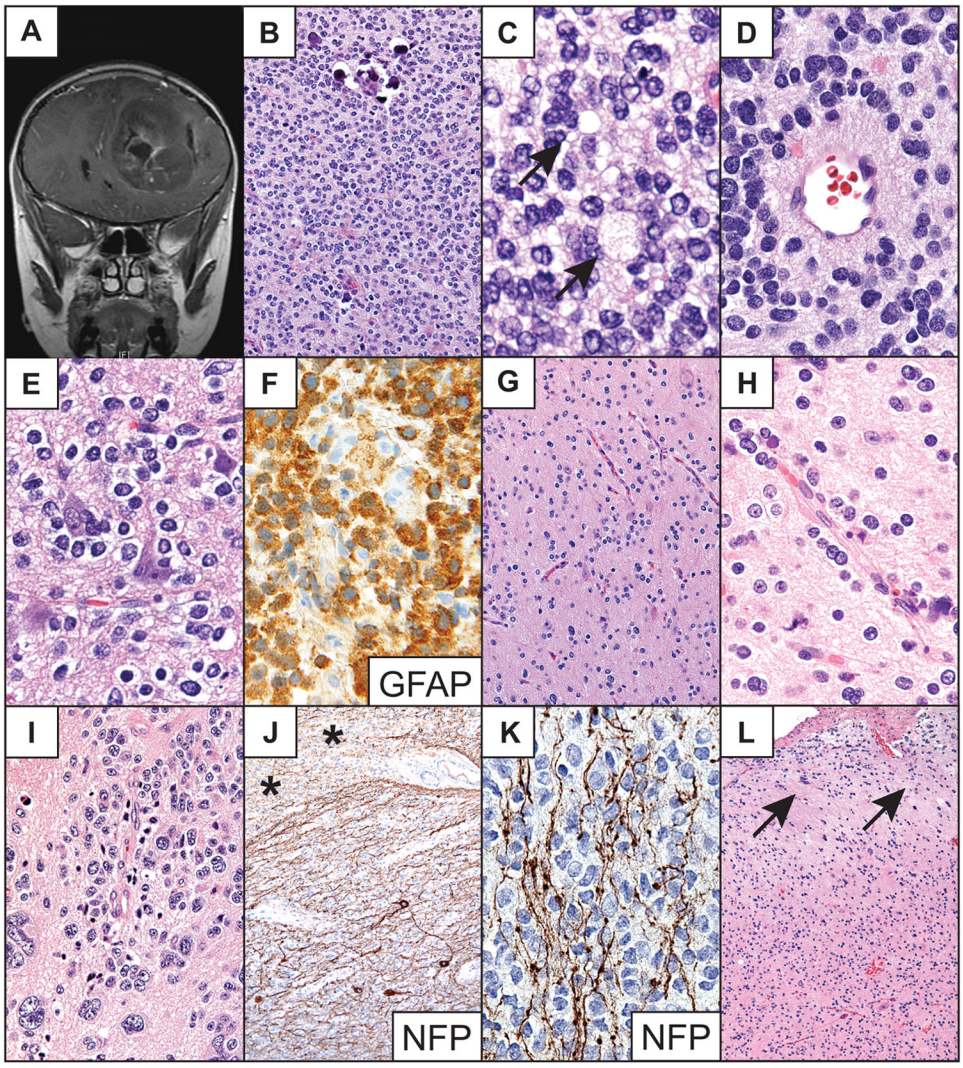

Fig 5.

Patient 5. **(A)** Post-contrast, T1-weighted image demonstrates a large deep left frontal tumor that extends to the cerebral cortex. **(B)** Large solid areas of the tumor are highly cellular and scattered calcospherites are present. **(C)** Occasional true ependymal rosettes are present in the solid areas of the tumor (arrows). **(D)** Scattered perivascular pseudorosettes are also observed. **(E)** Cortical field demonstrates the clear cell histology features and perineuronal satellitosis. **(F)** Tumor cells display strong glial fibrillary acidic protein (GFAP) immunoreactivity. **(G, H)** Tumor cells infiltrate the cortex freely and along small vessels in the cortex and other peripheral areas of the tumor. **(I)** Focal giant cell change is demonstrated in areas of nonrosetting angiocentric growth. **(J)** Neurofilament protein (NFP) immunostain shows the tumor in apparent transition from the cerebral white matter (asterisks) into the cerebral cortex. **(K)** NFP immunostain showing tumor cells infiltrating between nerve fibers within the cortex. **(L)** Subpial tumor cell mounding (arrows) is less dense in this specimen than in other cases. Routine stains are hematoxylin and eosin. Original magnifications: **(B, G)** 200×; **(C–F, H, K)** 600×; **(I)** 400×; **(J, L)** 100×.

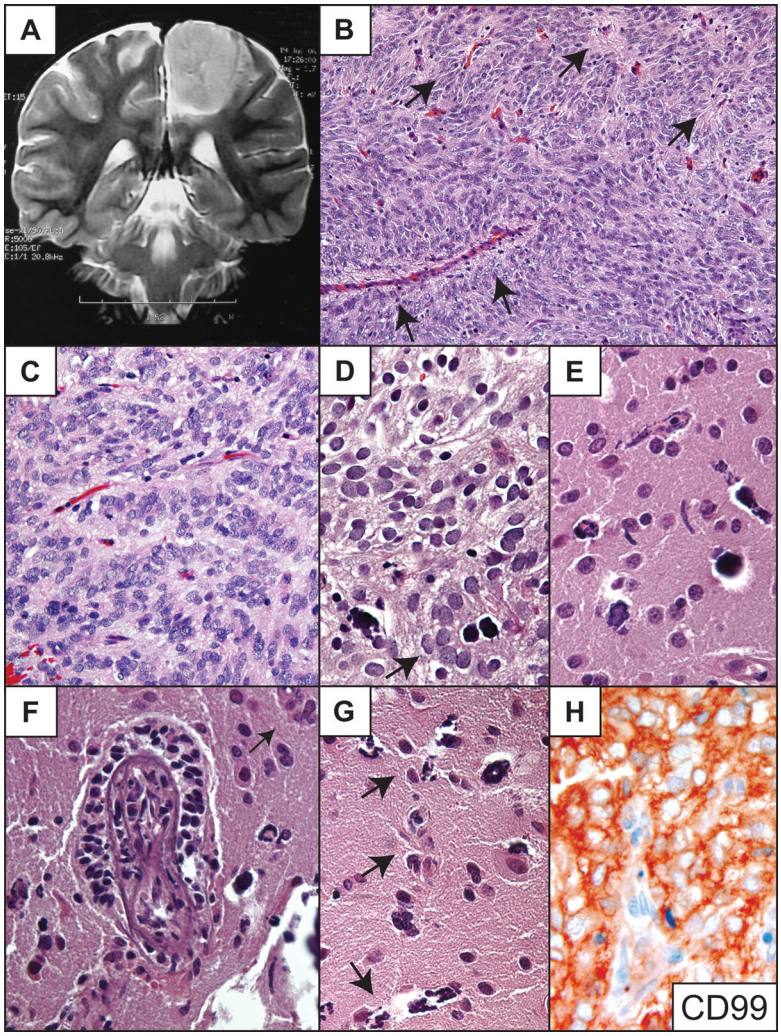

Fig 6.

Patient 6. **(A)** T2-weighted MRI showing the hyperintense solid tumor. **(B)** The densely cellular lesion had only vague perivascular pseudorosettes (arrows). **(C)** Higher-power view of vague pseudorosettes. **(D)** High-power photomicrograph shows clear cell features. There is a small perivascular pseudorosette with a mineralized central vessel in this field (arrow). **(E–G)** Freely infiltrating tumor cells within the cerebral cortex. Some display angiocentricity (arrows). Tumor cells were observed focally within the Virchow-Robin space **(F)**. Perineuronal satellitosis was also occasionally present **(F, G). (H)** The tumor showed strong diffuse immunopositivity for CD99. Hematoxylin and eosin stains, except **(H)**. Original magnifications: **(B)** 200×; **(C)** 400; **(D–H)** 600×.

J Neuropathol Exp Neurol. Author manuscript; available in PMC 2010 January 12.

Table

Summary of Cases*

No.	Age*/Sex	WHO Grade	Location*	Ki-67**	Treatment	Recurrence
1	11/M	I	R Frontal Cortex	< 1%	Surgery	None at 7 yr
2	1/F	III	R Frontal Cortex	80%	Surgery	None at 4 yr
3	24/M	I	R Amygdala	<1%	Surgery	Recurred at 1 yr, lost to follow-up
4	2/M	II	R Temporal Lobe	3%	Surgery + Radiation†	None at at 2 yr
5	8/M	III	L Frontal Lobe	20%	Surgery + Radiation†	None at 1 yr
6	8/F	II	L Frontoparietal Lobe	10%	Surgery x2, + Radiation†	Recurred at 4 yr, now 2 yr without (6 yr since diagnosis)

*Abbreviations: Age in years at initial clinical presentation; M, male; F, female; R, right; L, left; yr, years after surgical treatment

**Ki-67 labeling index (see Methods)

†Local field radiation therapy.